The Astrophysical Journal Letters, 826:L1 (7pp), 2016 July 20 doi:10.3847/2041-8205/826/1/L1

LOST AND FOUND: EVIDENCE OF SECOND-GENERATION STARS ALONG THE ASYMPTOTIC GIANT BRANCH OF THE GLOBULAR CLUSTER NGC 6752*

E. Lapenna[1,2], C. Lardo[3], A. Mucciarelli[1], M. Salaris[3], F. R. Ferraro[1], B. Lanzoni[1], D. Massari[2,4], P. B. Stetson[5], S. Cassisi[6], and A. Savino[3,4]
[1] Dipartimento di Fisica e Astronomia, Alma Mater Studiorum Università di Bologna, Viale Berti Pichat 6/2, I-40127 Bologna, Italy
[2] INAF–Osservatorio Astronomico di Bologna, Via Ranzani 1, I-40127 Bologna, Italy
[3] Astrophysics Research Institute, Liverpool John Moores University, 146 Brownlow Hill, Liverpool L3 5RF, UK
[4] Kepteyn Astronomical Institute, University of Groningen, Landleven 12, 9747 AD Groningen, The Netherlands
[5] National Research Council, 5071 West Saanich Road, Victoria, BC V9E 2E7, Canada
[6] INAF–Osservatorio Astronomico di Teramo, via Mentore Maggini, I-64100 Teramo, Italy
Received 2016 June 16; revised 2016 June 29; accepted 2016 June 29; published 2016 July 13

ABSTRACT

We derived chemical abundances for C, N, O, Na, Mg, and Al in 20 asymptotic giant branch (AGB) stars in the globular cluster (GC) NGC 6752. All these elements (but Mg) show intrinsic star-to-star variations and statistically significant correlations or anticorrelations analogous to those commonly observed in red giant stars of GCs hosting multiple populations. This demonstrates that, at odds with previous findings, both first- and second-generation (SG) stars populate the AGB of NGC 6752. The comparison with the Na abundances of red giant branch stars in the same cluster reveals that SG stars (with mild Na and He enrichment) do reach the AGB phase. The only objects that are not observed along the AGB of NGC 6752 are stars with extreme Na enhancement. This is also consistent with standard stellar evolution models, showing that highly Na and He enriched stars populate the bluest portion of the horizontal branch and, because of their low stellar masses, evolve directly to the white dwarf cooling sequence, skipping the AGB phase.

Key words: globular clusters: individual (NGC 6752) – stars: abundances – stars: AGB and post-AGB – techniques: spectroscopic

1. INTRODUCTION

The vast majority of Galactic globular clusters (GCs) host multiple stellar populations (MPs) characterized by different abundance ratios of selected light elements (see, e.g., Gratton et al. 2012 for a review): some stars share the same light element abundance ratios measured in Galactic field stars with similar metallicity, but a large fraction of the cluster population has enhanced N, Na, and Al and depleted C and O abundances. The patterns are not random, but anticorrelated variations of the pairs C–N and O–Na are commonly observed. These are generally considered to arise from hot hydrogen burning in a previous generation of more massive stars, as asymptotic giant branch (AGB) stars (Ventura & D'Antona 2005), fast-rotating massive stars (Decressin et al. 2007), interacting massive binary stars (De Mink et al. 2009), and/or supermassive stars (Denissonkov & Hartwick 2014).[7] Objects with standard composition are commonly denoted as first-generation (FG) stars, and those with modified chemistry as second-generation (SG) stars, although the assumption that they are formed in subsequent star formation episodes is sometimes questioned (see, e.g., Bastian et al. 2013).

In a few GCs the SG/FG star ratio measured along the red giant branch (RGB) is observed to differ from that measured along the AGB, with a substantial deficiency of SG stars within the AGB population, compared to the RGB (Norris et al. 1981; Gratton et al. 2010b; Campbell et al. 2012, 2013; Johnson et al. 2015; Lapenna et al. 2015; MacLean et al. 2016). In principle, this can be explained by taking into account that stars with evolving masses below $0.55 M_{\odot}$ are expected to fail reaching the AGB phase (the so-called *AGB-manqué* stars; see, e.g., Greggio & Renzini 1990) and SG stars are indeed expected to have a lower mass along the HB with respect to FG stars. In fact, since they are typically He-enhanced, they originate from RGB stars with a lower mass and end up, on average, with a lower mass along the HB, if the RGB mass loss is approximately the same for FG and SG sub-populations (see, e.g., Cassisi & Salaris 2013). One therefore expects that the AGB of GCs with a blue HB should lack at least part of the SG component, compared to what is seen along the RGB. This is consistent with the findings of Gratton et al. (2010b), who empirically showed that the number ratio between AGB and HB stars (the R_2 parameter) correlates with the HB morphology, in the sense that clusters with the bluest HB morphology have lower R_2 values.

NGC 6752 is a metal-intermediate GC with an extreme blue HB morphology and a low R_2 value, and it is claimed to be the most extreme case of a GC lacking SG stars along the AGB. In fact, Campbell et al. (2013, hereafter C13) measured the Na abundance of 20 AGB stars in this cluster and from the derived [Na/Fe] distribution; they concluded that all objects belong to the FG population. In their interpretation, the SG stars fail to reach the AGB phase because their HB progenitors are all located at effective temperatures ($T_{\rm eff}$) hotter than the Grundahl Jump (at ~11,500 K) and experience a very strong mass loss (a factor of 20 larger than that suffered along the RGB).[8] An alternative solution has been proposed by Charbonnel et al. (2013), who argued that the lack of SG AGB stars can be explained within the fast-rotating massive stars scenario by

* Based on observations collected at the ESO-VLT under the program 095.D-0320(A).

[7] We refer the reader to Renzini et al. (2015) for a critical analysis of the various scenarios for the polluters.

[8] We note that this assumption is at odds with the constraints from the stellar wind models for HB stars provided by Vink & Cassisi (2002).

assuming very high He abundances (up to $Y \sim 0.7$) for the SG objects, that therefore become *AGB-manqué* stars. On the other hand, by using detailed synthetic HB simulations, Cassisi et al. (2014) were able to reproduce the star distribution along the HB of NGC 6752 and its observed R_2 value assuming the initial He-abundance distribution derived from the cluster main sequence (Y between ∼0.25 and ∼0.27; see Milone et al. 2013) without invoking any extreme HB mass loss or initial He enhancement. However, these simulations show that ∼50% of the AGB population should be composed of SG stars, at odds with the claim by C13.

With the aim of solving this intriguing issue, here we present the chemical abundances of iron and several light elements that we recently determined from high-resolution spectra for the same sample of AGB stars discussed in C13.

2. OBSERVATIONS

The 20 AGB stars in NGC 6752 previously studied by C13 have been re-observed (program 095.D-0320(A), PI: Mucciarelli) with the UVES spectrograph (Dekker et al. 2000) mounted at the ESO-Very Large Telescope. We used the Dichroic1 mode adopting the gratings 390 Blue Arm CD#2 and 580 Red Arm CD#3 with the 1 arcsec slit ($R = 40{,}000$). Exposure times range from ∼10 minutes for the brightest targets to ∼25 minutes for the faintest ones to obtain pixel signal-to-noise ratios higher than 100. The data reduction was performed by using the dedicated ESO pipeline, including bias subtraction, flat fielding, wavelength calibration, spectral extraction, and order merging.

3. CHEMICAL ANALYSIS

The chemical analysis has been performed following the same procedure described in Lapenna et al. (2015). The stellar atmospheric parameters have been derived as follows:

1. $T_{\rm eff}$ have been derived spectroscopically by requiring no trend between iron abundances and excitation potentials.
2. Surface gravities ($\log g$) have been obtained through the Stefan–Boltzmann relation, adopting the spectroscopic $t_{\rm eff}$, the distance modulus $(m-M)_0 = 13.13$ and color excess $E(B-V) = 0.04$ (Ferraro et al. 1999), and a mass of 0.61 $M_\odot$, according to the median value of the HB mass range estimated by Gratton et al. (2010a).[9] Stellar luminosities have been calculated using the bolometric corrections by Alonso et al. (1999) and the V-band magnitudes from the ground-based photometric catalog reduced and calibrated following the procedures described in Stetson (2000, 2005).
3. Microturbulent velocities (v_t) have been obtained by requiring no trend between iron abundances and line strengths.

The derived values of $T_{\rm eff}$ and v_t agree well with those by C13, with average differences $\Delta T_{\rm eff} = +31 \pm 8$ K and $\Delta v_t = -0.03 \pm 0.01$ km s^{-1}. For $\log g$ there is a systematic difference $\Delta \log g = +0.220 \pm 0.005$ dex, probably due to the different distance modulus and the larger stellar mass adopted by C13.

The abundances of Fe, Na, Mg, and Al have been derived using the classical method of the equivalent widths (EWs) with the package GALA (Mucciarelli et al. 2013b).[10] EWs have been measured by means of the DAOSPEC package (Stetson & Pancino 2008), iteratively launched with the code 4DAO (Mucciarelli 2013).[11] The linelist was built using a synthetic reference spectrum calculated at the UVES resolution and selecting only transitions predicted to be unblended. We adopted the atomic data of the last release of the Kurucz/Castelli compilation[12] for all species except for Fe II lines, which have been taken from Meléndez & Barbuy (2009). The adopted model atmospheres have been computed with the ATLAS9 code[13] adopting a global metallicity of $[{\rm M/H}] = -1.5$ dex. The abundances of Na have been corrected for NLTE effects according to Gratton et al. (1999) and consistently with the analysis of C13. For seven stars the Al lines at 6696–6698 Å are too weak to be detected and only upper limits can be obtained.

The abundances of C, N, and O have been measured through the spectral synthesis technique, using the forbidden oxygen line at 6300 Å, and the CH and CN molecular bands at 4300 and 3880 Å, respectively. To derive the abundance of N we have taken into account the abundance of carbon measured from the CH band, while for the O abundance we adopted the average C and N abundances thus obtained, together with the measured abundance of Ni. This was done to take into account the close blending of the O line at 6300 Å with a Ni transition. We also checked that the O transition is free from telluric contamination in 19 out of 20 AGB stars. For the star 1620 the contamination is severe and we did not derive the O abundance.

As reference solar abundances, we assumed those of Grevesse & Sauval (1998), except for C, N, and O, for which we assumed the values of Caffau et al. (2011).

The computation of the final abundance uncertainties adds in quadrature two terms. The first is the error arising from spectral feature measurements. For the abundances derived from EWs, this term is obtained for each star by dividing the line-to-line dispersion by the square root of the number of lines used. For the elements analyzed with spectral synthesis, the fitting procedure is repeated for a sample of 500 synthetic spectra where Poissonian noise has been injected to reproduce the noise conditions (see Mucciarelli et al. 2013a). The second term is the abundance error arising from atmospheric parameters. This has been computed by varying each parameter by its 1σ uncertainty obtained in the analysis. Due to the quality of the spectra we found that the typical internal uncertainties for $T_{\rm eff}$ are lower than ∼35 K, while for $\log g$ and v_t we found values lower than 0.1 dex and 0.05 km s^{-1}, respectively.

4. RESULTS

4.1. Iron Abundances

The derived iron abundance ratios are listed in Table 1 together with the stellar atmospheric parameters. We obtain average $[{\rm Fe\,I/H}] = -1.80 \pm 0.01$ dex ($\sigma = 0.05$ dex) and

[9] Cassisi et al. (2014) derived a slightly lower (∼0.55 $M_\odot$) median mass. The adoption of this value decreases $\log g$ by ∼0.04, with a negligible impact on the abundances, ∼0.02 for [Fe II/H] and smaller than 0.01 dex for the other species.

[10] http://www.cosmic-lab.eu/gala/gala.php
[11] http://www.cosmic-lab.eu/4dao/4dao.php
[12] http://wwwuser.oats.inaf.it/castelli/linelists.html
[13] http://wwwuser.oats.inaf.it/castelli/sources/atlas9codes.html

Table 1
Atmospheric Parameters and Abundance Ratios of the Analyzed AGB Stars in NGC 6752

ID	$T_{\rm eff}$ (K)	log g (dex)	v_t (km s^{-1})	[Fe I/H] (dex)	[Fe II/H] (dex)	[C/Fe] (dex)	[N/Fe] (dex)	[O/Fe II] (dex)	[Na/Fe] (dex)	[Mg/Fe] (dex)	[Al/Fe] (dex)
22	4554	1.18	1.85	–1.77 ± 0.01	–1.61 ± 0.01	–0.29 ± 0.07	+1.20 ± 0.12	+0.41 ± 0.01	+0.29 ± 0.04	+0.37 ± 0.01	+0.52 ± 0.02
25	4351	0.92	1.80	–1.79 ± 0.01	–1.60 ± 0.01	–0.25 ± 0.06	+0.68 ± 0.12	+0.54 ± 0.06	–0.00 ± 0.03	+0.44 ± 0.01	<–0.11
31	4413	1.06	1.85	–1.76 ± 0.01	–1.56 ± 0.01	–0.17 ± 0.07	+0.76 ± 0.12	+0.53 ± 0.04	–0.03 ± 0.01	+0.38 ± 0.03	<–0.22
44	4585	1.31	1.65	–1.79 ± 0.01	–1.58 ± 0.01	–0.17 ± 0.07	+0.73 ± 0.12	+0.49 ± 0.05	–0.01 ± 0.03	+0.40 ± 0.01	<–0.21
52	4752	1.55	1.65	–1.81 ± 0.01	–1.61 ± 0.02	–0.19 ± 0.08	+0.99 ± 0.13	+0.44 ± 0.04	+0.14 ± 0.02	+0.41 ± 0.01	+0.20 ± 0.03
53	4712	1.44	1.70	–1.78 ± 0.01	–1.59 ± 0.01	–0.34 ± 0.08	+1.29 ± 0.13	+0.23 ± 0.02	+0.22 ± 0.02	+0.38 ± 0.01	+0.40 ± 0.03
59	4724	1.50	1.65	–1.81 ± 0.01	–1.58 ± 0.01	–0.34 ± 0.08	+1.29 ± 0.13	+0.21 ± 0.01	+0.25 ± 0.01	+0.38 ± 0.01	+0.34 ± 0.05
60	4690	1.44	1.65	–1.68 ± 0.01	–1.55 ± 0.01	–0.09 ± 0.07	+0.72 ± 0.13	+0.56 ± 0.05	–0.10 ± 0.03	+0.36 ± 0.02	<–0.21
61	4722	1.50	1.70	–1.77 ± 0.01	–1.58 ± 0.01	–0.19 ± 0.08	+0.99 ± 0.13	+0.44 ± 0.05	+0.17 ± 0.02	+0.42 ± 0.01	+0.36 ± 0.03
65	4622	1.31	1.80	–1.81 ± 0.01	–1.59 ± 0.01	–0.41 ± 0.07	+1.32 ± 0.13	+0.21 ± 0.01	+0.35 ± 0.03	+0.40 ± 0.01	+0.52 ± 0.03
75	4724	1.55	1.65	–1.84 ± 0.01	–1.59 ± 0.01	–0.10 ± 0.08	+0.68 ± 0.13	+0.48 ± 0.03	–0.05 ± 0.01	+0.38 ± 0.02	<–0.21
76	4862	1.64	1.70	–1.84 ± 0.01	–1.61 ± 0.01	–0.42 ± 0.08	+1.30 ± 0.13	+0.25 ± 0.05	+0.30 ± 0.04	+0.42 ± 0.02	+0.54 ± 0.05
78	4877	1.65	1.75	–1.82 ± 0.01	–1.58 ± 0.01	–0.46 ± 0.08	+1.40 ± 0.13	+0.16 ± 0.03	+0.32 ± 0.03	+0.38 ± 0.01	+0.53 ± 0.04
80	4804	1.63	1.70	–1.80 ± 0.01	–1.58 ± 0.01	–0.18 ± 0.08	+0.91 ± 0.13	+0.39 ± 0.02	+0.05 ± 0.02	+0.43 ± 0.01	<–0.28
83	4817	1.63	1.60	–1.85 ± 0.01	–1.59 ± 0.01	–0.16 ± 0.08	+1.08 ± 0.13	+0.38 ± 0.02	+0.19 ± 0.02	+0.36 ± 0.01	+0.33 ± 0.05
89	4798	1.63	1.65	–1.86 ± 0.01	–1.58 ± 0.01	–0.34 ± 0.08	+1.15 ± 0.13	+0.28 ± 0.02	+0.30 ± 0.02	+0.38 ± 0.01	···
94	4864	1.71	1.65	–1.88 ± 0.01	–1.56 ± 0.02	–0.37 ± 0.08	+1.26 ± 0.13	+0.17 ± 0.03	+0.24 ± 0.04	+0.39 ± 0.01	+0.20 ± 0.05
97	4884	1.75	1.70	–1.89 ± 0.01	–1.58 ± 0.01	–0.33 ± 0.08	+1.14 ± 0.13	+0.22 ± 0.06	+0.25 ± 0.01	+0.40 ± 0.01	+0.15 ± 0.06
104	4753	1.66	1.60	–1.87 ± 0.01	–1.54 ± 0.01	–0.16 ± 0.08	+0.73 ± 0.13	+0.40 ± 0.07	+0.01 ± 0.03	+0.42 ± 0.01	<–0.03
1620	4902	1.71	1.70	–1.80 ± 0.01	–1.56 ± 0.01	–0.26 ± 0.08	+1.19 ± 0.14	···	+0.23 ± 0.01	+0.38 ± 0.02	+0.18 ± 0.04

Note. Identification number (from C13), $T_{\rm eff}$, log g, v_t, and abundance ratios for Fe I, Fe II, C, N, O, Na, Mg, and Al.

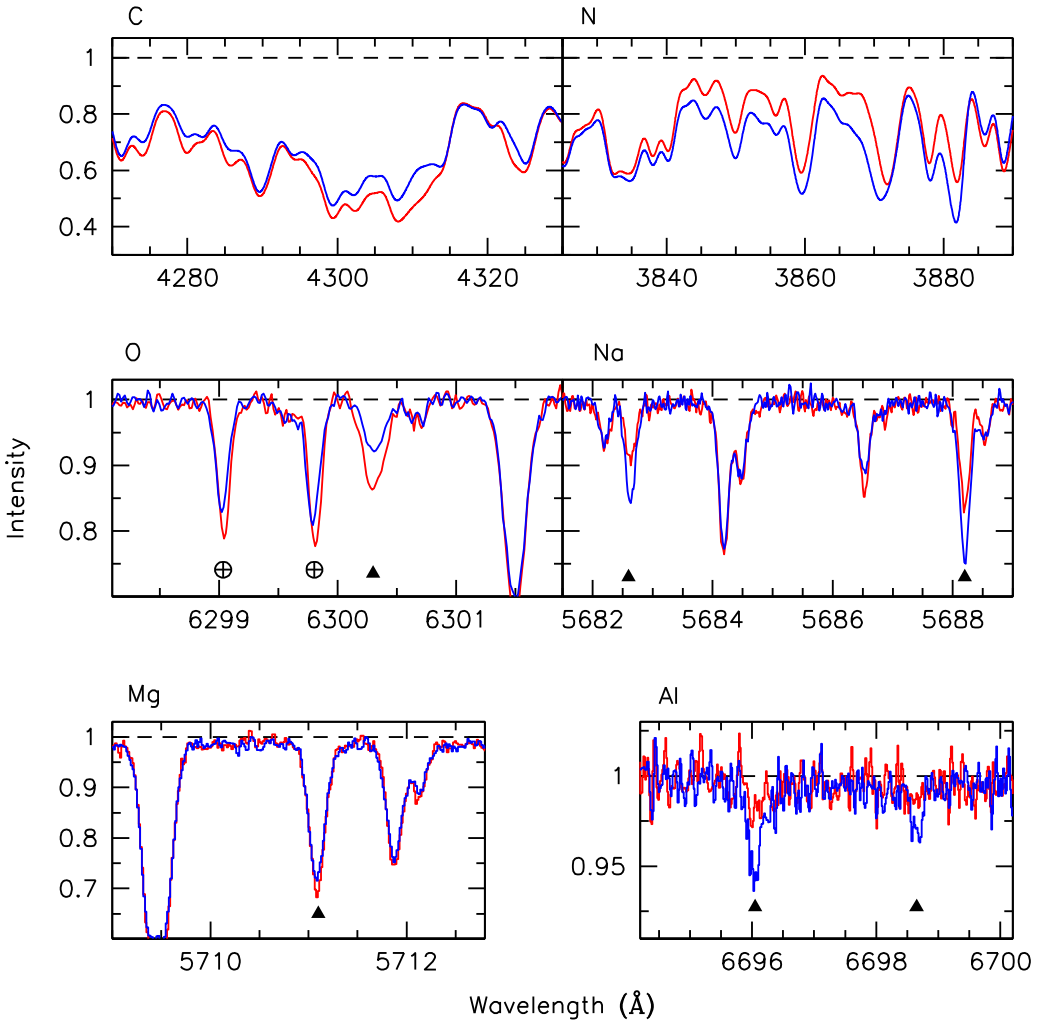

Figure 1. Comparison between the spectra of the AGB stars 44 (blue line) and 65 (red line) in the spectral regions around the atomic and molecular features used in this work (and marked with arrowheads). The black dashed line marks the continuum position. In each panel, the black crossed-circles highlight the position of two telluric lines.

[Fe II/H] $= -1.58 \pm 0.01$ dex ($\sigma = 0.02$ dex). The average [Fe II/H] abundance is consistent with the values measured in RGB stars by Yong et al. (2003), Gratton et al. (2005), and Carretta et al. (2007, 2009a), while [Fe I/H] is 0.22 dex lower than the metallicity inferred from Fe II lines. Such a discrepancy between [Fe I/H] and [Fe II/H] among AGB stars is too large to be explained within internal uncertainties and has been observed previously in other GCs (Ivans et al. 2001; Lapenna et al. 2014, 2015; Mucciarelli et al. 2015a, 2015b). The same [Fe I/H]–[Fe II/H] discrepancy remains also if we adopt the atmospheric parameters quoted in C13. Note that C13 do not measure directly the Fe abundance, but assume the average RGB [Fe/H] by Carretta et al. (2007) for all the targets. With their atmospheric parameters we derive [Fe I/H] $= -1.77 \pm 0.01$ dex ($\sigma = 0.05$ dex) and [Fe II/H] $= -1.50 \pm 0.01$ dex ($\sigma = 0.02$ dex). Even if a complete explanation of this effect is still lacking, this *iron discrepancy* seems to be a general feature of AGB stars in GCs.

4.2. Light Elements

Significant inhomogeneities in the light element abundances of the studied AGB stars are immediately apparent already from the visual inspection of the acquired spectra. This can be appreciated in Figure 1, where the CH and CN molecular bands, and O, Na, Mg, and Al lines of star 44 and star 65 (having very similar atmospheric parameters; see Table 1) are compared. Apart from Mg, notable differences in the line strength are well visible for all the other elements. Moreover, the strength of the C and O features appears to anticorrelate with the strength of the N and Na lines. This clearly shows that the two stars are highly inhomogeneous in their light element content.

The abundance ratios obtained for the entire AGB sample are listed in Table 1. Following the approach discussed in Ivans et al. (2001) and Lapenna et al. (2015), the abundance ratios have been computed by adopting [Fe I/H] as the reference except for O, for which we used [Fe II/H]. This method provides the best agreement between the abundance ratios in AGB and RGB stars of the same cluster. However, because the origin of the Fe I–Fe II discrepancy is still unclear, we will discuss the abundances of AGB stars with respect to both hydrogen and iron to ensure that our results are independent of the adopted normalization of the abundance ratios. With the only exception of Mg, for which we find values confined within a narrow range, the abundances of all the other light elements show dispersions well exceeding the internal errors (see

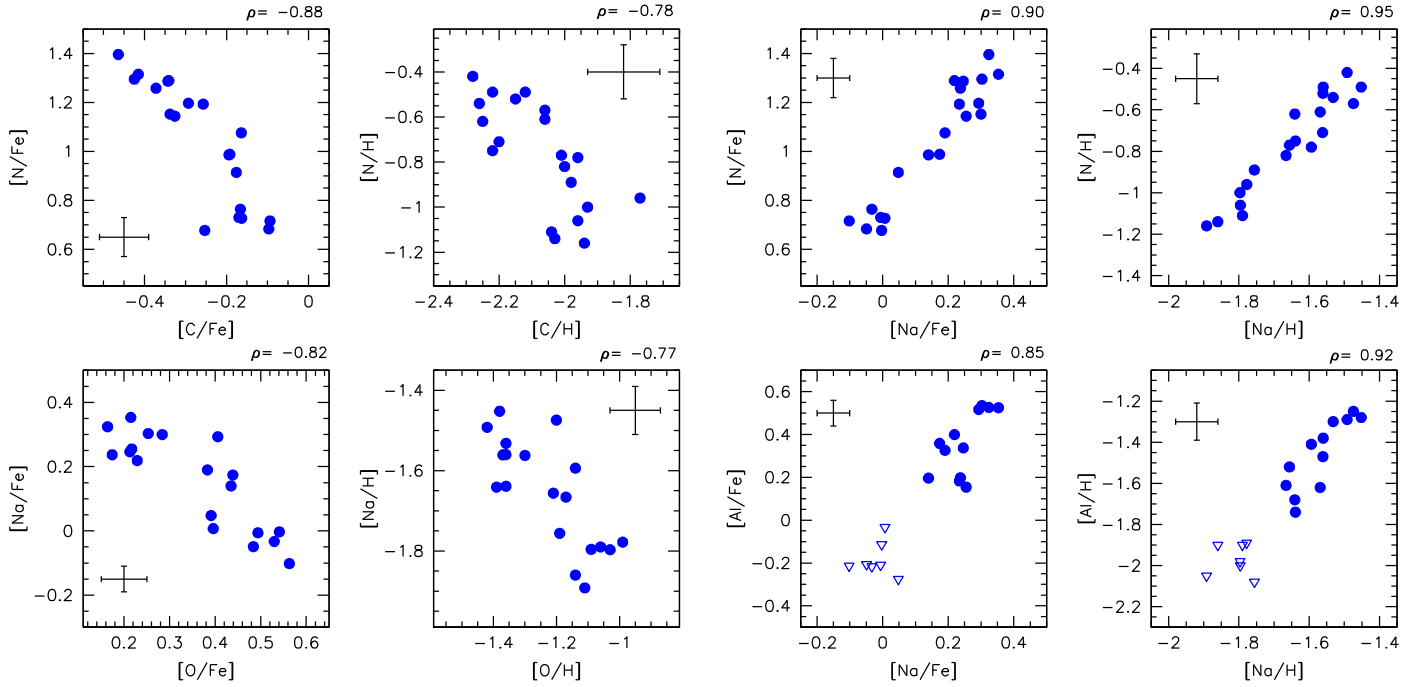

Figure 2. Light element abundances measured for the investigated AGB stars. All abundance ratios are shown normalized both to iron and to hydrogen. The typical error bars of the measured abundances and the the Spearman rank coefficients of every correlation are marked in each panel. In the bottom right panels the empty triangles mark the stars for which only upper limits to [Al/Fe] have been derived.

Table 1). This is true not only for the abundance ratios referred to iron, but it also holds for normalizations to hydrogen. In particular, the measured sodium abundances span a range of Δ[Na/Fe]$\simeq\Delta$[Na/H] $\simeq$ 0.45, for nitrogen we find Δ[N/Fe] $\simeq$ Δ[N/H] $\simeq$ 0.8, and for oxygen we obtain Δ[O/Fe] $\simeq$ Δ[O/H] $\simeq$ 0.4.

The detected inhomogeneities also appear to be mutually correlated. In fact, Figure 2 shows clear C–N and O–Na anticorrelations, and N–Na and Na–Al correlations, both if we consider the abundance ratios referred to Fe and if we normalize to H. In all cases, the statistical significance, as measured by the Spearman rank coefficients $|\rho|$, is very high (values of $|\rho|$ larger than 0.74 corresponds to non-correlation probabilities lower than $\sim 10^{-4}$). In these diagrams, star 44 and star 65 (see Figure 1) reside at two opposite ends, the former being C- and O-rich and N-, Na-, Al-poor, while star 65 shows a specular pattern. The existence of such well-defined correlations, by itself, indicates the presence of multiple sub-populations along the AGB of NGC 6752. By definition, in fact, a sample composed exclusively of FG stars (as suggested by C13) would display homogeneous abundances and produce no correlations. Indeed, the detected correlations are perfectly in agreement with those commonly ascribed to FG and SG sub-populations in GCs (see, e.g., Carretta et al. 2009a, 2009b).

5. DISCUSSION

Figure 3 shows the AGB population (solid blue circles) of NGC 6752 in the "standard" [Na/Fe]–[O/Fe] plane. For reference, we also plot the results obtained for the RGB population of NGC 6752 (empty red squares; from Yong et al. 2003) and several RGB samples in 19 GCs (gray dots; from Carretta et al. 2009b). The AGB population of NGC 6752 clearly outlines and follows the anti-correlation stream defined by the RGB samples, thus confirming the existence of SG AGB

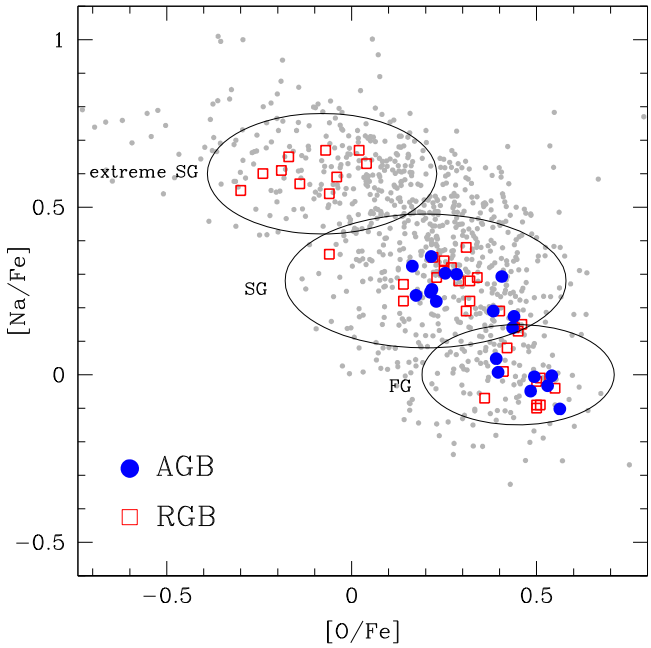

Figure 3. Behavior of [Na/Fe] as a function of [O/Fe] for the AGB (filled blue circles; this work) and RGB stars (open red squares; Yong et al. 2003) of NGC 6752. The results obtained for RGB stars in other GCs (Carretta et al. 2009b), rescaled to the solar values adopted in this work, are shown as gray dots for reference. The regions corresponding to the three populations identified by Milone et al. (2013, see their Figure 15) are encircled.

stars in NGC 6752. To better characterize the cluster sub-populations, in Figure 3 we also plot three ellipses corresponding to the values of [Na/Fe] and [O/Fe] that Milone et al. (2013), on the basis of their photometric study and the chemical abundances measured by Yong et al. (2003), associate to the FG, SG, and extreme-SG sub-samples in NGC 6752

("Populations a, b, and c" in their nomenclature; see Figure 15 in Milone et al. 2013). Notably, the abundances here determined for the AGB population nicely match the FG and SG loci, thus demonstrating that, at odds with the claim by C13, SG stars also experience the AGB phase in NGC 6752. In particular, based on Table 1 and Figure 3, we count 13 (out of 20) SG stars, corresponding to ∼65% of the total AGB sample investigated here.

Following Milone et al. (2013), the FG stars in NGC 6752 have a standard chemical mixture ($Y \sim 0.24$), SG stars have a moderate enhancement of [Na/Fe] and He ($Y \sim 0.25$) and a mild depletion of [O/Fe], and extreme-SG stars have high [Na/Fe] and He ($Y \sim 0.27 - 0.28$) and low [O/Fe]. Our results show that the AGB sample is composed of the first two populations only, while the extreme-SG stars are not observed. Nicely, the SG/(FG+SG) fraction estimated photometrically by Milone et al. (2013) is ∼64%, in very good agreement with the value (65%) found here. The lack of the extreme-SG stars along the AGB is exactly what the synthetic HB simulations by Cassisi et al. (2014) predict. These simulations consider three stellar populations with initial He abundances equal to those quoted by Milone et al. (2013), and they are able to well reproduce the observed value of the R_2 parameter and the HB morphology, magnitude, and color distribution, without invoking exceptional mass loss during the HB phase. They predict that the extreme-SG is the most He-rich population, which populates the bluer end of the HB and produces *AGB-manqué* objects. Also, the observed fraction of FG AGB stars (35% of the total) is consistent, within the statistical fluctuations due to the small size of the sample, with the predictions (∼50%) of Cassisi et al. (2014).

Therefore, the observed fraction of failed AGB stars in NGC 6752 can be easily explained within the standard stellar evolution framework, with no need of invoking exceptional mass loss for HB stars hotter than the Grundahl jump (C13), or extremely high (and inconsistent with the photometric constraints from the main sequence) initial He abundances for the SG population (Charbonnel et al. 2013).

The results presented here provide firm evidence that the AGB population of NGC 6752 includes both FG and SG stars. While this is in line with similar results obtained from both spectroscopic (García-Hernández et al. 2015) and photometric (Milone et al. 2015a, 2015b; Nardiello et al. 2015) observations in various GCs, it is in contrast with the findings of C13.

Although a detailed discussion of the origin of the discrepancy with the result by C13 is beyond the scope of this Letter, a preliminary comparison between the two samples demonstrates that there is a systematic offset (Δ[Na/Fe] ∼ 0.25 dex) between the values of [Na/Fe] measured here and those measured by C13.[14] This is the main reason why while we count at least 11 stars above [Na/Fe] = 0.18 dex (the threshold adopted by C13); no stars were found by C13. On the other hand, the clear anticorrelations shown in Figure 2 for the entire set of light elements, clearly indicated the existence of SG stars along the AGB of NGC 6752, thus demonstrating that the chemical analysis of a single light element does not allow us to draw reliable conclusions about the presence or lack of SG populations. Indeed, the adoption of the classical scheme based on the analysis of light element (anti)correlations appears to be the most appropriate spectroscopic way to detect and distinguish FG and SG stars.

[14] We also note that C13 adopted a constant iron abundance for the entire sample. This can be dangerous in the case of AGB stars that suffer from the still unclear problem affecting the measure of neutral elemental abundances (see Ivans et al. 2001; Lapenna et al. 2014, 2015; Mucciarelli et al. 2015a, 2015b).

E.L. acknowledges the financial support from PRIN-INAF 2014. C.L. gratefully acknowledges financial support from the European Research Council (ERC-CoG-646928, Multi-Pop). D.M. has been supported by the FIRB 2013 (MIUR grant RBFR13J716). S.C. is grateful for financial support from PRIN-INAF 2014 (PI: S. Cassisi). We warmly thank the anonymous referee for useful comments, which improved the paper.

REFERENCES

Alonso, A., Arribas, S., & Martínez-Roger, C. 1999, A&AS, 140, 261
Bastian, N., Lamers, H. J. G. L. M., de Mink, S. E., et al. 2013, MNRAS, 436, 2398
Caffau, E., Ludwig, H.-G., Steffen, M., Freytag, B., & Bonifacio, P. 2011, SoPh, 268, 255
Campbell, S. W., D'Orazi, V., Yong, D., et al. 2013, Natur, 498, 198
Campbell, S. W., Yong, D., Wylie-de Boer, E. C., et al. 2012, ASPC, 458, 205
Carretta, E., Bragaglia, A., Gratton, R., & Lucatello, S. 2009a, A&A, 505, 139
Carretta, E., Bragaglia, A., Gratton, R. G., et al. 2009b, A&A, 505, 117
Carretta, E., Bragaglia, A., Gratton, R. G., Lucatello, S., & Momany, Y. 2007, A&A, 464, 927
Cassisi, S., & Salaris, M. 2013, Old Stellar Populations: How to Study the Fossil Record of Galaxy Formation (Weinheim: Wiley-VCH)
Cassisi, S., Salaris, M., Pietrinferni, A., Vink, J. S., & Monelli, M. 2014, A&A, 571, AA81
Charbonnel, C., Chantereau, W., Decressin, T., Meynet, G., & Schaerer, D. 2013, A&A, 557, LL17
Decressin, T., Meynet, G., Charbonell, C., Prantzos, N., & Ekstrom, S. 2007, A&A, 464, 1029
Dekker, H., D'Odorico, S., Kaufer, A., Delabre, B., & Kotzlowski, H. 2000, Proc. SPIE, 4008, 534
De Mink, S. E., Pols, O. R., Langer, N., & Izzard, R. G. 2009, A&A, 507L, 1
Denissonkov, P. A., & Hartwick, F. D. A. 2014, MNRAS, 437, 21
Ferraro, F. R., Messineo, M., Fusi Pecci, F., et al. 1999, AJ, 118, 1738
García-Hernández, D. A., Mészáros, S., Monelli, M., et al. 2015, ApJL, 815, L4
Gratton, R. G., Bragaglia, A., Carretta, E., et al. 2005, A&A, 440, 901
Gratton, R. G., Carretta, E., & Bragaglia, A. 2012, A&ARv, 20, 50
Gratton, R. G., Carretta, E., Bragaglia, A., Lucatello, S., & D'Orazi, V. 2010a, A&A, 517, 81
Gratton, R. G., Carretta, E., Eriksson, K., & Gustafsson, B. 1999, A&A, 350, 955
Gratton, R. G., D'Orazi, V., Bragaglia, A., Carretta, E., & Lucatello, S. 2010b, A&A, 522, 77
Greggio, L., & Renzini, A. 1990, ApJ, 364, 35
Grevesse, N., & Sauval, A. J. 1998, SSRv, 85, 161
Ivans, I. I., Kraft, R. P., Sneden, C., et al. 2001, AJ, 122, 1438
Johnson, C. I., McDonald, I., Pilachowski, C. A., et al. 2015, AJ, 149, 71
Lapenna, E., Mucciarelli, A., Ferraro, F. R., et al. 2015, ApJ, 813, 97
Lapenna, E., Mucciarelli, A., Lanzoni, B., et al. 2014, ApJ, 797, 124
MacLean, B. T., Campbell, S. W., De Silva, G. M., et al. 2016, MNRAS, in press (arXiv:1604.05040)
Meléndez, J., & Barbuy, B. 2009, A&A, 497, 611
Milone, A. P., Marino, A. F., Piotto, G., et al. 2013, ApJ, 767, 120
Milone, A. P., Marino, A. F., Piotto, G., et al. 2015a, ApJ, 808, 51
Milone, A. P., Marino, A. F., Piotto, G., et al. 2015b, MNRAS, 447, 927
Mucciarelli, A. 2013, arXiv:1311.1403
Mucciarelli, A., Bellazzini, M., Catelan, M., et al. 2013a, MNRAS, 435, 3667
Mucciarelli, A., Lapenna, E., Massari, D., et al. 2015a, ApJ, 809, 128
Mucciarelli, A., Lapenna, E., Massari, D., Ferraro, F. R., & Lanzoni, B. 2015b, ApJ, 801, 69
Mucciarelli, A., Pancino, E., Lovisi, L., Ferraro, F. R., & Lapenna, E. 2013b, ApJ, 766, 78
Nardiello, D., Piotto, G., Milone, A. P., et al. 2015, MNRAS, 451, 312
Norris, J., Cottrell, P. L., Freeman, K. C., & Da Costa, G. S. 1981, ApJ, 244, 205
Renzini, A., D'Antona, F., Cassisi, S., et al. 2015, MNRAS, 454, 4197
Stetson, P. B. 2000, PASP, 112, 925

Stetson, P. B. 2005, PASP, 117, 563
Stetson, P. B., & Pancino, E. 2008, PASP, 120, 1332
Ventura, P., & D'Antona, F. 2005, ApJL, 635, L149
Vink, J. S., & Cassisi, S. 2002, A&A, 392, 553
Yong, D., Grundahl, F., Lambert, D. L., Nissen, P. E., & Shetrone, M. D. 2003, A&A, 402, 985